Supporting Information

Serio et al. 10.1073/pnas.1103516108

SI Materials and Methods

Expression Vectors and Antibodies. The plasmid YFP-Rab5A was provided by A. Sorkin (University of Pittsburgh, Pittsburgh, PA). pBABEGFP-H2B was from Mario Faretta (European Institute of Oncology, Milan, Italy), and pTAGRFP–α-tubulin was from EVROGEN. For the ablation/reconstitution experiments, the inducible silencing-resistant Rab5A plasmid was generated by recombinant PCR mutating 3 nt in the sequence targeted by the silencing oligo without affecting the amino acid sequence and cloned in the tetracycline-inducible vector pSG213 (gift from G. Draetta, Belfer Institute for Applied Cancer Science, Boston, MA). The Rab5 dominant-negative mutant, Rab5AS34N, was tagged with myc and cloned in pSG213.

Antibodies used were mouse monoclonal anticentrin 20H5 (provided by J. L. Salisbury, Mayo Clinic, Rochester, MN), anti–CENP-F (gift from S. Taylor, Manchester, United Kingdom), mouse monoclonal anti-Rab5A (clone 1, 610724; Becton Dickinson), mouse antipan-Rab5 (HPA003426; Sigma-Aldrich), mouse monoclonal anti–c-myc (9E10 sc-40; Santa Cruz), rabbit polyclonal anti-Rab21 antibody (H00023011-M01; Novus Biologicals), rabbit polyclonal anti–γ-tubulin (T3559; Sigma-Aldrich), mouse monoclonal anti–γ-tubulin (clone GTU-88, T6557; Sigma-Aldrich), rabbit polyclonal anti–α-tubulin (ab15246; Abcam), rabbit polyclonal anti–CENP-F (ab5; Abcam), mouse monoclonal anti–CENP-E (clone 1H12, ab5093; Abcam), human anticentromere antibody ACA (Antibodies Incorporated), mouse monoclonal anti-HEC1 (clone 9G3.23; Genetex), rabbit polyclonal anti–β-tubulin (H-235; Santa Cruz), rabbit polyclonal antilamin B1 (ab16048; Abcam), goat polyclonal antilamin B (C-20, sc-6216; Santa Cruz), rabbit polyclonal anti-H3(phosphoS10) (ab 5176; Abcam), and mouse monoclonal anti-H3(phosphoS10) (clone 6G3, 9706; Cell Signaling).

Immunoprecipitation Experiments. U2OS cells stably expressing YFP-Rab5A were synchronized at mitosis by treatment with 50 ng/mL nocodazole (Sigma) overnight. Mitotic cells were collected by mitotic shake off, washed two times with cold PBS, and lysed in cold JS buffer (50 mM Hepes, pH 7.5, 150 mM NaCl, 1% glycerol, 1% Triton X-100, 1.5 mM $MgCl_2$, 5 mM EGTA) plus proteases and phosphatases inhibitors (20 mM sodium pyrophosphate, 100 μg/mL Aprotinin, 100 μg/mL Leupeptin, 50 mM NaF, 2 mM PMSF, 10 mM sodium orthovanadate). Lysates were cleared by centrifugation (30 min at 10,000 × *g*). Total cellular lysates (3 mg) were incubated with rabbit polyclonal anti-GFP Sepharose-conjugated antibody (ab69314; Abcam) for 2 h at 4 °C. Immunoprecipitates were washed four times with lysis buffer, boiled for 5 min in Laemmli buffer, and run on a SDS/PAGE gradient gel (4–15%; Bio-Rad) followed by immunoblotting.

Time-Lapse Experiments. Time lapse of cells stably expressing YFP-Rab5A and RFP–α-tubulin was done with an UltraVIEW VoX spinning disk confocal unit (PerkinElmer) equipped with an inverted Nikon Eclipse Ti microscope and a Yokogawa CSU-X1 scanning head driven by Volocity software (Improvision; PerkinElmer). In Movie S1, *Z* stacks were captured every 5 min with a 60× oil-immersion objective (N.A. = 1.4), and step size was 0.6 μm. In Movie S2, frames of a single section were captured every 600 ms with a 60× oil immersion objective (N.A. = 1.4).

We quantified the frequency of Rab5 vesicles at spindles in 13 movies of metaphase U2OS cells expressing YFP-Rab5A and RFP–α-tubulin. These movies result from *Z* projection of seven sections (corresponding to 3 μm) taken in the equatorial region of the spindle; *Z* stacks were acquired every 3 s for ∼4 min. Movie S3 is a representative movie used in the quantification. Quantification of Rab5 vesicles was done with ImageJ applying a mask corresponding to the spindle area to each time point. The frequency of Rab5 vesicles at spindles represents the percent of vesicles found within the spindle relative to their total number at each time point.

For the analysis on the mitotic behavior of silenced cells, time lapse of U2OS cells stably expressing H2B-GFP and RFP–α-tubulin, silenced either with control oligos or Rab5A, -B, or -C oligos, was performed using a Leica AF6000LX fluorescent workstation. Silenced cells were plated into glass-bottomed dishes (WillCo-dish; Willcowells) and placed onto a sample stage within an incubator chamber set at 37 °C in an atmosphere of 5% CO_2 and 20% humidity. Images were captured with a 40× objective using 200-ms exposure time for both channels every 5 min for 10 h and keeping the lamp intensity at minimum to avoid phototoxicity. *Z*-stacks images were collected every 0.6 μm on a cell thickness around 10 μm. Automated acquisition of at least 15 different fields for each sample was done by using a high-precision motorized stage. Deconvolved images and *Z* projections were generated with the LAS AF Leica Application Suite software (Leica).

Immunofluorescence. Cells were grown on glass coverslips coated with 0.5% gelatin, fixed in 4% formaldehyde for 10 min at room temperature, permeabilized in PBS, 0.2% BSA, and 0.1% Triton X-100 for 10 min at room temperature, and blocked in PBS 3% BSA for 30 min at room temperature. For cells stained with anti–γ-tubulin, centrin and CENP-E antibodies fixation/extraction was performed with cold (−20 °C) methanol for 1 min on ice. Primary antibodies were revealed by Alexa Fluor 555-, 488- (Molecular Probes), or Cy5- (Jackson) conjugated secondary antibodies. Confocal analysis was performed on a Leica TCS SP2 AOBS microscope. Maximum projection of images was created from *Z* stacks (step interval = 0.13–0.5 μm) and processed in Adobe Photoshop.

Immunofluorescence Intensity Analysis and in Situ Proximity Ligation Assay. Quantification of kinetochores intensity was done by confocal acquisition of *Z* stacks with the identical number of sections and settings. Quantification was performed on the average of *Z*-stack projections using ImageJ. Briefly, an ellipsoidal region was centered on each kinetochore, and ACA intensity was measured in the same region and used for normalization after subtraction of background intensity measured outside the cell. For the quantification of CENP-F at kinetochores, the gain and offset parameters were kept stringent enough to minimize the contribution of diffuse CENP-F staining not corresponding to kinetochores. Fluorescence intensity of lamin B1 and CENP-F at nuclear envelope was measured on a single confocal section for each cell acquired with identical settings. Measurements were done as described in ref. 1 by determining pixel intensities along 4-μm lines that start 3 μm away from the nuclear envelope using the quantification tool Profile of Leica Confocal software. Mean intensities were calculated for 10 lines in each cell. In situ proximity ligation assays were performed with the Duolink kit purchased from Olink Bioscience according to the manufacturer's instructions.

Measurements of Interkinetochore Distance and Centrosome–Nuclear Periphery Distance. We measured the interkinetochore distance of kinetochore pairs on confocal sections in which both sister kinetochores were on the same focal plane using the quantification tool Profile (line) of Leica Confocal software.

Mean distances between the nuclear periphery and each of the two centrosomes were measured on confocal *Z* projections using the quantification tool Profile (line) of Leica Confocal software.

Kinetochore Microtubule Stability. U2OS-silenced cells were treated with 10 μM MG132 for 2 h, washed with cold PBS, chilled at 4 °C for 10 min in DMEM supplemented with 20 mM Hepes, and fixed and stained with anti–α-tubulin and ACA antibodies. Deconvolution microscopy was performed using a wide-field optical sectioning Leica AF6000LX fluorescent workstation (Leica). *Z* series of images taken at 0.1-μm intervals by means of a piezoelectric device mounted between the objective and the turret were captured with a 63× objective and processed with 10 rounds of iterative deconvolution. Figures were generated by projecting sum of the optical sections. Deconvolution and projection were done with the LAS AF Leica Application Suite software (Leica).

1. Li H, et al. (2010) Polo-like kinase 1 phosphorylation of p150Glued facilitates nuclear envelope breakdown during prophase. *Proc Natl Acad Sci USA* 107:14633–14638.

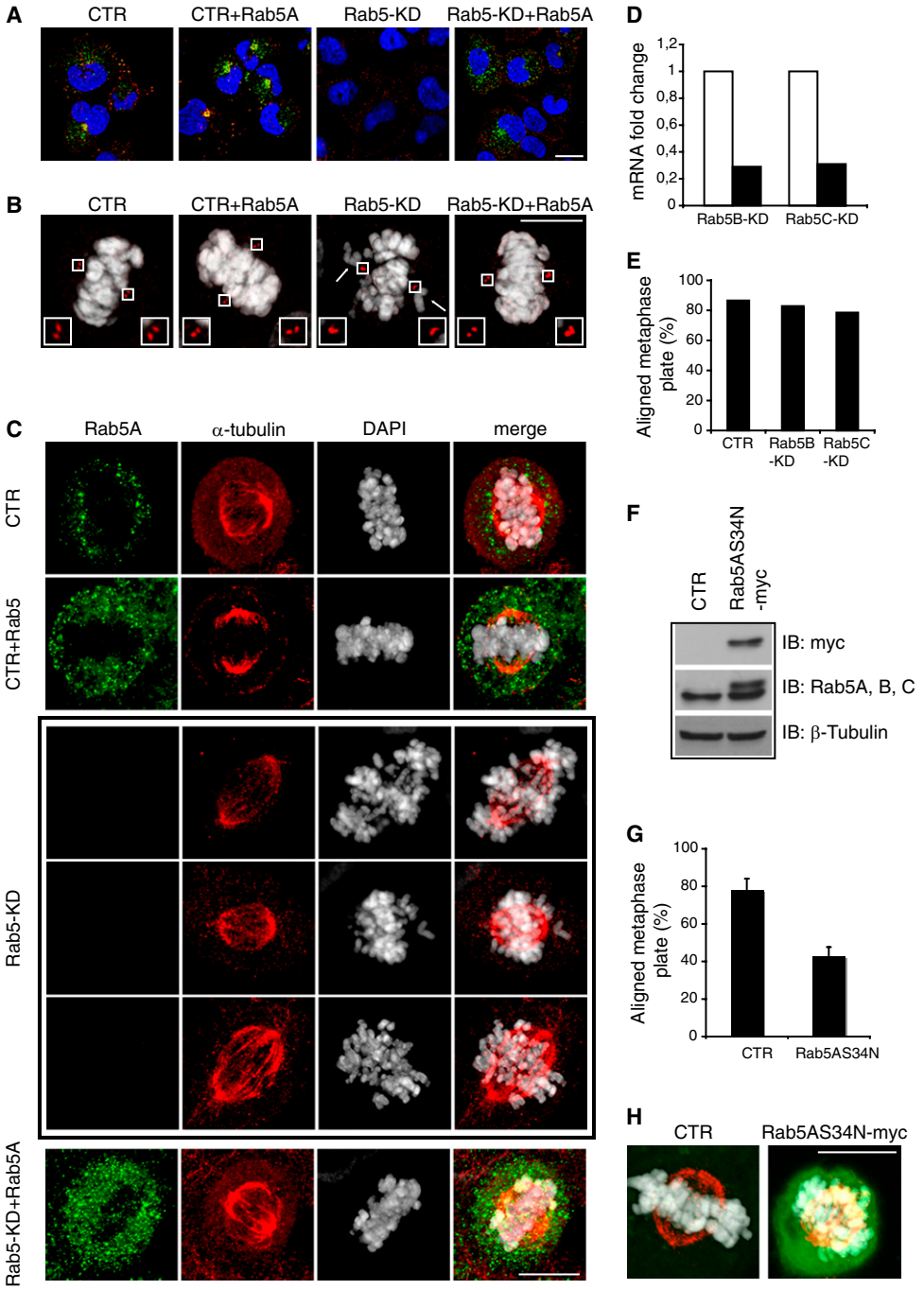

Fig. S1. (*A*) U2OS cells, silenced and treated as shown along the top, were serum-starved for 2 h. After starvation, cells were incubated in DMEM plus 5 μg/mL Transferrin Alexa Fluor 555-conjugated (Invitrogen) and BSA 0.2% for 1 h on ice and then shifted at 37 °C for 10 min before fixation. Merged images show Alexa Fluor 555-conjugated transferrin in red, Rab5A in green and DAPI in blue. (*B*) U2OS cells, silenced and treated as listed along the top, were stained with anticentrin antibody (red) and DAPI (gray). Arrows point to misaligned chromosomes in the Rab5-silenced cell. Chromosome congression is rescued by expression of Rab5A in the Rab5-silenced cell. Spindle poles are boxed and magnified in *Insets*. (*C*) *Z* projections of confocal images of metaphase-arrested cells from the experiments in Fig. 2*B*. Cells silenced and treated as on the left were stained with anti-Rab5A (green), anti–α-tubulin (red) antibodies, and DAPI (gray). Merged images are also shown. Three examples of Rab5-knockdown (Rab5-KD) cells with different degrees of chromosome uncongression are shown. They represent, respectively, 18 ± 2%, 39 ± 6%, and 43 ± 4% of the total aberrant mitotic Rab5-KD cells ($n = 3$, 200 cells/experiment). (*D*) U2OS cells were transiently transfected with control siRNA oligos or oligos for Rab5B (Rab5B-KD) or Rab5C (Rab5C-KD), and they were analyzed for mRNA content by quantitative RT-PCR. mRNA content in Rab5B-KD or Rab5C-KD (black bars) is expressed as fold change with respect to control RNAi-transfected cells (white bars). (*E*) Cells silenced as in *D* were treated with MG132 for 2 h and stained with anti–α-tubulin antibody and DAPI. The bar graph represents the quantification of metaphase-arrested cells with aligned chromosomes. (*F*) U2OS cells stably transfected with the tetracycline-inducible TET ON construct for Rab5AS34N-myc were mock-treated (CTR) or treated with doxycycline (Rab5AS34N-myc; 2.5 μg/mL doxycycline for 48 h). Total cellular lysates were immunoblotted (IB) as indicated. (*G*) Cells as in *F* were treated with MG132 for 2 h and stained with anti–α-tubulin, anti-myc antibodies, and DAPI. The bar graph represents the quantification of metaphase-arrested cells with aligned chromosomes. Mean values ± SD ($n = 3$, 100 cells/condition per experiment) are shown. *P* value = 0.0017. (*H*) Representative confocal pictures of cells in *G*. Merged images show myc (Rab5AS34N) in green, α-tubulin in red, and DAPI in gray.

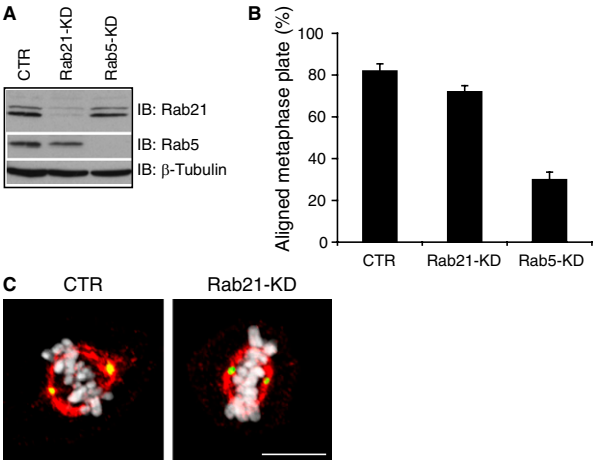

Fig. S2. Functional ablation of Rab21 does not affect chromosome congression. (*A*) Total cellular lysates from cells silenced as shown along the top were IB as indicated. (*B*) U2OS cells silenced with control oligos (CTR), Rab21-oligos (Rab21-KD), or Rab5-oligos (Rab5-KD) were treated with MG132 for 2 h and stained with anti–α-tubulin antibody and DAPI. The bar graph represents the quantification of metaphase-arrested cells with aligned chromosomes. Mean values ± SD (n = 3, 100 cells/condition per experiment) are shown. (*C*) Representative confocal images from the experiments in *B* are shown, anti–α-tubulin (red), anti–γ-tubulin (green), and DAPI (gray) stainings are merged.

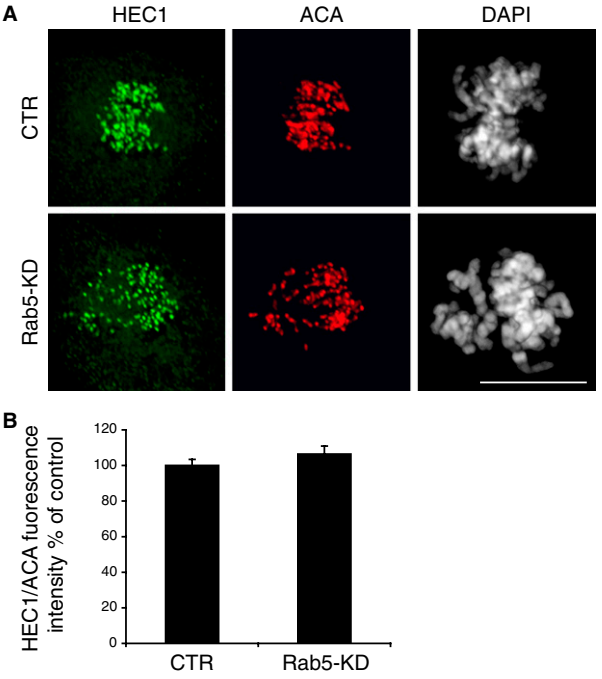

Fig. S3. HEC1, a subunit of the Ndc80 complex, localizes to kinetochores in Rab5-silenced cells. (*A*) Confocal *Z* projections of cells silenced as indicated on the left and stained with anti-HEC1 (green), ACA (red) antibodies, and DAPI (gray). (*B*) Quantification of pixel intensity (percent of control) showing that HEC1 localization to kinetochores is unaffected in Rab5-silenced cells. Values represent the mean ± SEM of 30 well-resolved kinetochores in three different cells.

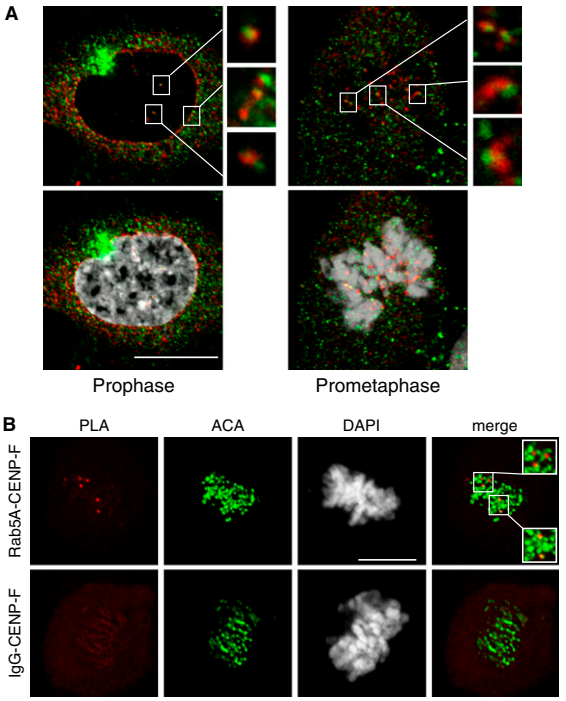

Fig. S4. Localization of Rab5 and CENP-F in mitotic cells. (*A*) Single confocal sections of U2OS cells at prophase and prometaphase (indicated along the bottom) stained with anti-Rab5A (green), anti–CENP-F (red) antibodies, and DAPI (gray). *Upper* shows the merging of Rab5 and CENP-F stainings, and *Lower* also includes DAPI. Some regions showing overlap between Rab5 and CENP-F were boxed in *Upper* and magnified in *Insets*. (*B*) Confocal *Z* projections of mitotic U2OS cells showing is PLA signals in cells incubated with anti-Rab5A and anti–CENP-F antibodies (*Upper*) or control cells where the anti-Rab5 antibody was substituted with purified mouse IgG (*Lower*). is PLA signal (red) and ACA staining (green) are also shown in the merge column, and DAPI is in gray. Positive signals are boxed in the merge column and magnified in *Insets*. No signals are detectable in the control cell; 4.5 is PLA signals were detected in Rab5A–CENP-F cells vs. 0.25 is PLA signals in IgG–CENP-F cells (n = 2 10 cells/condition).

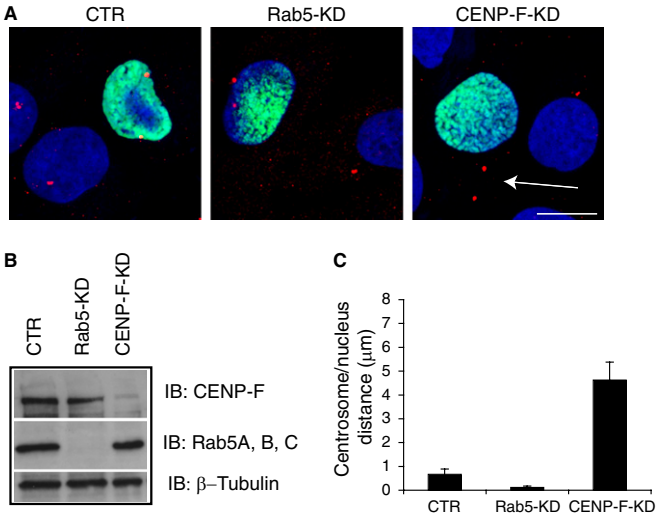

Fig. S5. Depletion of Rab5 does not impair centrosome tethering to the nuclear envelope. (*A*) Confocal *Z* projections of cells silenced as reported along the top and stained with anti–α-tubulin (red), anti-H3(phosphoS10) (green) antibodies, and DAPI (blue). Arrow points at detached centrosomes in the cell depleted of CENP-F. (*B*) Total cellular lysates of U2OS cells silenced as reported along the top were IB as indicated. (*C*) The bar graph represents the quantification of the distances between centrosomes and nuclear periphery measured in cells silenced and stained as in *A*. Mean values of distances expressed in micrometers ± SD are shown (n = 3, ≥17 cells/condition). *P* value CENP-F–KD vs. control = 0.0001.

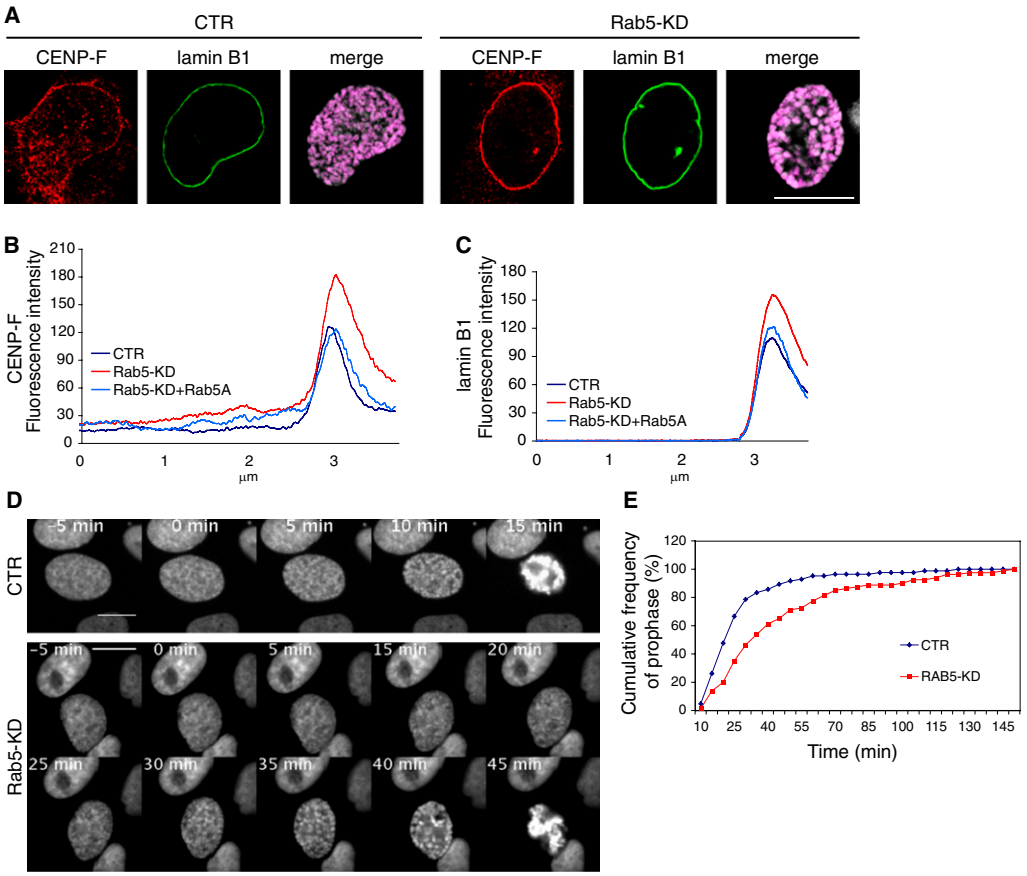

Fig. S6. Depletion of Rab5 retards nuclear envelope disassembly and increases the levels of CENP-F and lamin B1 at the nuclear envelope. (*A*) Single confocal sections of U2OS cells at prophase, silenced as indicated along the top, were stained with anti–CENP-F (red), antilamin B1 (green), anti-H3(phosphoS10) (magenta) antibodies, and DAPI (gray). Stainings of phospho-H3 and DAPI are merged. The fluorescence intensity of both CENP-F and lamin B1 is increased in the Rab5-silenced cell compared with the control cell. (*B* and *C*) The graph lines represent the mean fluorescence intensity of CENP-F (*B*) or lamin B1 (*C*) measured in cells silenced with control oligos (CTR; blue line) or in cells silenced with Rab5 oligos and either mock-treated (Rab5-KD; red line), or treated with doxycycline to reexpress Rab5A (Rab5-KD + Rab5A; light blue line; $n = 2 \geq 7$ cells/condition). *P* value for graph line (*B*) = 0.0009. *P* value for graph line (*C*) = 0.001. (*D*) Selected frames of a single section from movies of cells stably expressing H2B-GFP silenced with control oligos (CTR; *Top*) or Rab5-oligos (Rab5-KD; *Bottom*) showing the duration of prophase. Time is in minutes; $t = 0$ is defined as the time point at which chromosome condensation becomes evident. (*E*) Cumulative frequency plot showing the time spent in prophase; 84 cells in control (CTR; blue line) and 80 cells in Rab5-KD (red line) were analyzed. *P* value = 6.99×10^{-05}.

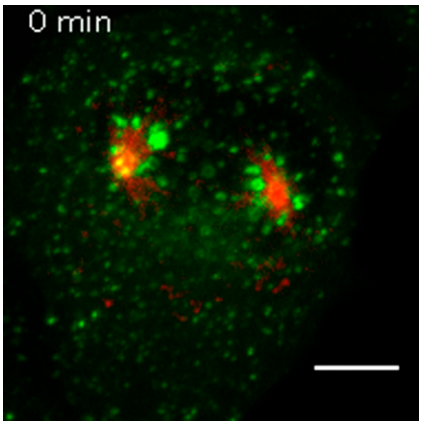

Movie S1. Rab5 dynamics during mitosis. This movie shows a mitotic U2OS cell expressing YFP-Rab5A (green) and RFP–α-tubulin (red) during spindle assembly from prophase to cytokinesis. Frames were captured every 5 min; $t = 0$ was defined as the point at which the spindle starts to assemble. The movie results from *Z* projection of 13 sections. Playback is 1 frame/s.

Movie S1

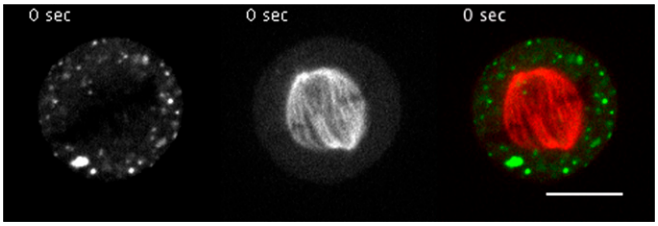

Movie S2. Rab5 vesicles move within the spindle at metaphase. This movie shows a U2OS cell expressing YFP-Rab5A (green) and RFP–α-tubulin (red) at metaphase. Frames of a single section taken in the equatorial region of the spindle were captured every 600 ms. Time is shown in seconds. Playback is 7 frames/s.

Movie S2

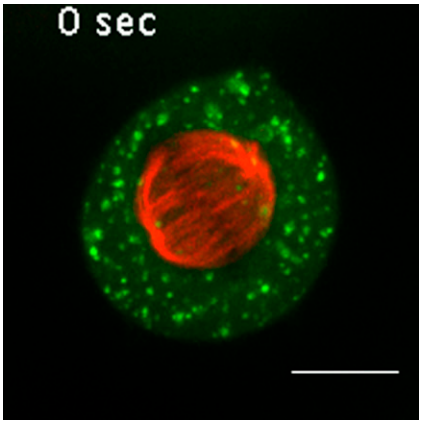

Movie S3. Localization of Rab5 vesicles during metaphase. This movie shows a U2OS cell expressing YFP-Rab5A (green) and RFP–α-tubulin (red) at metaphase. *Z* stacks corresponding to 3 μm within the spindle were captured every 3 s. Time is shown in seconds. Playback is 7 frames/s.

Movie S3

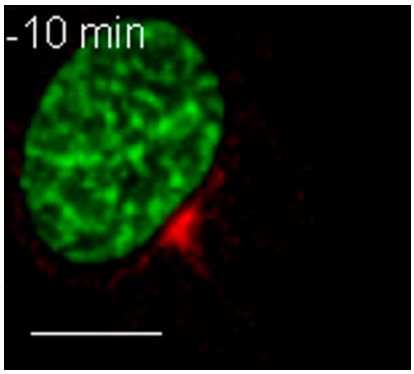

Movie S4. Spindle assembly and chromosome movements in control cells. This movie shows a mitotic U2OS cell expressing H2B-GFP (green) and mRFP–α-tubulin (red) silenced with control oligos. Frames were captured every 5 min. Time is in minutes; $t = 0$ corresponds to late prophase. Selected frames have been presented in Fig. 2*C*. Playback is 3 frames/s.

Movie S4

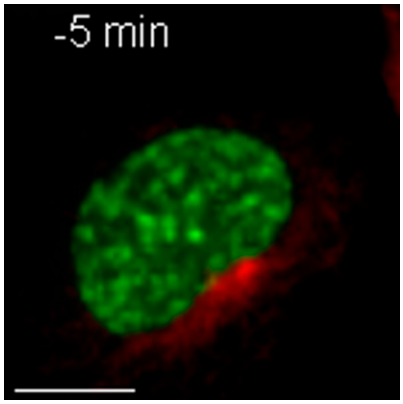

Movie S5. Spindle assembly and chromosome movements in an Rab5-silenced cell. This movie shows a mitotic U2OS cell expressing H2B-GFP (green) and mRFP–α-tubulin (red) silenced with Rab5 oligos. Frames were captured every 5 min. Time is in minutes; $t = 0$ corresponds to late prophase. This cell displays defects in chromosome congression and a strong delay in the onset of anaphase. Selected frames have been presented in Fig. 2*D*. Playback is 3 frames/s.

Movie S5

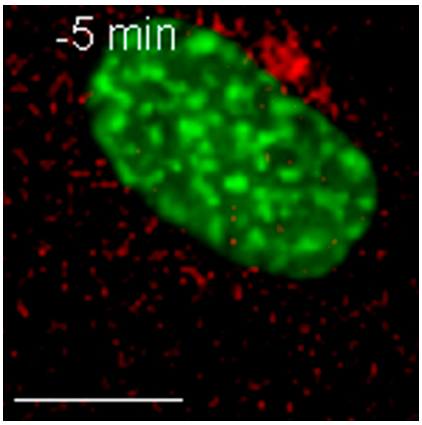

Movie S6. Chromosome missegregation in an Rab5-silenced cell. Mitotic U2OS cell expressing H2B-GFP (green) and mRFP–α-tubulin (red) silenced with Rab5 oligos. Frames were captured every 5 min. Time is in minutes. $t = 0$ corresponds to late prophase. This movie shows a Rab5-silenced cell undergoing anaphase with uncongressed chromosomes. Playback is 3 frames/s.

Movie S6

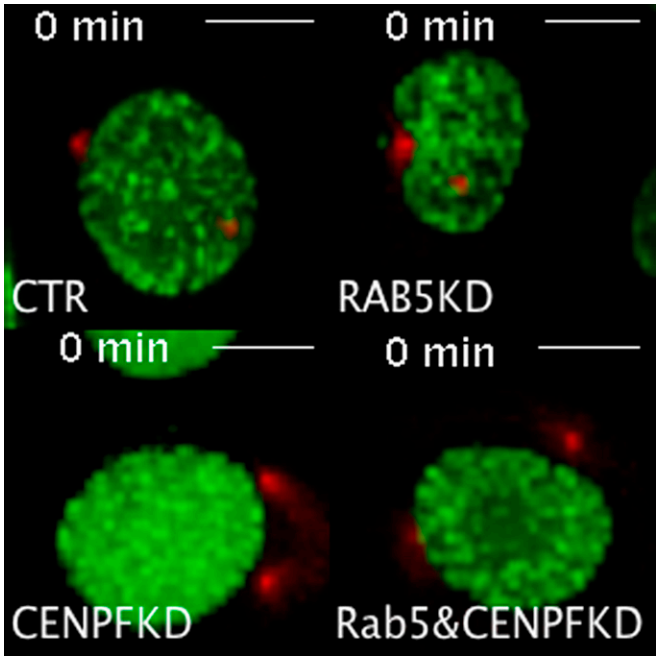

Movie S7. Spindle assembly, chromosome congression, and segregation in cells depleted of either or both Rab5 and CENP-F. U2OS cells expressing H2B-GFP (green) and mRFP–α-tubulin (red) silenced as indicated in the first frame filmed from prophase to cytokinesis. Frames were captured every 5 min. Time is in minutes. Playback is 7 frames/s. Chromosome alignment defects and mitotic delay are comparable in the cells silenced for either or both Rab5 and CENP-F.

Movie S7